01 Apr 2014

Peritidal Carbonate Cycles Induced by Carbonate Productivity Variations: A Conceptual Model for an Isolated Early Triassic Greenhouse Platform in South China

Wan Yang
Missouri University of Science and Technology, yangwa@mst.edu

Daniel J. Lehrmann

Recommended Citation

W. Yang and D. J. Lehrmann, "Peritidal Carbonate Cycles Induced by Carbonate Productivity Variations: A Conceptual Model for an Isolated Early Triassic Greenhouse Platform in South China," *Journal of Palaeogeography*, vol. 3, no. 2, pp. 115-126, China University of Petroleum Beijing, Apr 2014.
The definitive version is available at https://doi.org/10.3724/SP.J.1261.2014.00047

Journal of Palaeogeography
2014, 3(2): 115−126
DOI: 10.3724/SP.J.1261.2014.00047

Lithofacies palaeogeography and sedimentology

Peritidal carbonate cycles induced by carbonate productivity variations: A conceptual model for an isolated Early Triassic greenhouse platform in South China

Wan Yang[1, *], Dan J. Lehrmann[2]

1. Geology and Geophysics Program, Missouri University of Science and Technology, Rolla, Missouri 65409, USA
2. Department of Geosciences, Trinity University, San Antonio, TX 78212, USA

Abstract Eustasy has commonly been invoked to explain peritidal carbonate cyclicity, but is difficult to explain cycles formed in a greenhouse climate when eustasy is minimal. We propose that peritidal cycles on an Early Triassic isolated carbonate platform in Guizhou, South China, were formed by hierarchical carbonate productivity variations. Most of the 149 shallowing-upward cycles are typically terminated by flooding over intertidal facies and contain rare supratidal facies and no prolonged subaerial exposure. Low-diversity benthos in the platform interior during the post-end-Permian biotic recovery were sensitive to environmental perturbations, which caused variations in benthic sediment productivity in the subtidal carbonate factory. The perturbations may be driven by changes in salinity and degree of eutrophication, or repeated platform mini-drowning by anoxic and/or CO_2-charged deep water upwelled onto the banktop. They were modulated by Milankovitch orbitally-driven climatic and oceanographic factors as suggested by the hierarchical stacking pattern and spectral signals of these cycles. A one-dimensional conceptual model shows that hierarchical productivity variations alone may generate hierarchical peritidal carbonate cycles under conditions of constant subsidence and no sea-level fluctuation.

Key words carbonate, peritidal, cycle, productivity, climate, Triassic, South China

1 Introduction

Shallowing-upward peritidal carbonate cycles result from interplay of allogenic and autogenic processes controlling accommodation space and sediment accumulation (*e.g.*, Goldhammer *et al.*, 1990, among many others). The former is controlled by eustasy and subsidence (*e.g.*, Read and Goldhammer, 1988), the latter by factors affecting carbonate productivity and sediment redistribution, such as water depth, biota, salinity, oxygenation, nutrient, and current energy (cf. Tucker *et al.*, 1990; Schlager, 2005). Three mechanisms, all assuming constant subsidence and sedimentation, are commonly suggested for peritidal cycle formation: composite eustasy (*e.g.*, Goldhammer *et al.*, 1990), tidal flat sediment accumulation and progradation (*e.g.*, Ginsburg, 1971; Pratt and James, 1986), and random processes (*e.g.*, Spencer and Demicco, 1989; Drummond and Wilkinson, 1993a; Wilkinson *et al.*, 1999; Burgess, 2001, 2008), among which only Milankovitch-related composite eustasy can generate multi-order hierarchical cycles. In this study, we explore the link between carbonate productivity and cyclicity on the basis of sedimentary and quantitative evidence of peritidal cycles in South China.

* Corresponding author. E-mail: yangwa@mst.edu.
Received: 2013−08−20 Accepted: 2013−12−18

2 Characteristics of peritidal carbonate cycles

The peritidal carbonate cycles described here are suitable to explore the role of carbonate productivity variations on peritidal cyclicity, because they developed during the Early Triassic (Induan) greenhouse period when eustasy was minimal (Frakes *et al.*, 1992; Scotese *et al.*, 1999) and the benthic biota recovering from the end-Permian mass extinction was highly sensitive to varying oceanic conditions. They were deposited on an isolated flat-topped carbonate bank, which covers 10×70 km^2 in the eastern Paleo-Tethys (Figure 1A, 1B; Lehrmann *et al.*, 1998). It was named as the Great Bank of Guizhou by Lehrmann (1993) and as the Luodian Carbonate Platform by Feng *et al.* (1997). The bank has a low-relief profile with oolite shoals at the margin, shallow-subtidal and peritidal deposits in the interior, and pelagics, debris-flow deposits and turbidites on gentle basin-margin slopes (Figure 1C). Interior strata are 265 m thick beginning in the lowermost Triassic with *Renalcis* biostromes, followed by lime mudstone, oolite, and cyclic peritidal carbonate.

The cyclic carbonate is Olenekian in age. Two sections, Dajiang (DJ) on the windward side and Dawen (DW) toward the leeward side, are 140 m and 162 m thick, respectively (Figure 1C). They contain a total of 149 cycles that range from 0.2 to 7.4 m thick and are 2 m thick on average (Figures 1C, 2A, 2B). A typical cycle consists of four facies (Figure 2C; Lehrmann *et al.*, 1998, 2001): subtidal skeletal packstone or oolitic grainstone in the lower part, calcimicrobial *Renalcis* mound or biostrome facies in the middle, and intertidal flaser-bedded ribbon-rock facies in the upper part, all of which are pyritiferous. The skeletal packstone and reef mounds contain a low-diversity biota of cyanobacteria, echinoderms, bivalves, gastropods, lingulid brachiopods, spirorbids, and ostracodes. Ribbon rocks contain alternating lime mud and fine peloidal packstone and grainstone laminae, scour surfaces, ripple cross-lamination, lime-mud drapes, and minor prism cracks. Rarely, cycles are capped by supratidal microbial laminite facies, which account for only 2% of the section thickness. Overall, the facies were deposited in a dominantly low-energy, restricted- to normal-marine peritidal environment. The facies stacking suggests a shallowing-upward trend of depositional environments within each cycle, upward from high-energy shallow subtidal, relatively deep low-energy subtidal, to intertidal and, rarely, supratidal (see Lehrmann *et al.*, 1998, 2001 for thorough descriptions and interpretations).

Furthermore, cycle (parasequence) stacking patterns show gradual increase and decrease of cycle thickness, defining a third-order sequence boundary and several fourth-order cycle sets that correlate between DJ and DW sections (Figures 2, 3A; Lehrmann *et al.*, 2001). Lehrmann *et al.* (2001) stated that the cycle stacking patterns are similar to those of lower Paleozoic green-house sequences and different from those of ice-house sequences. They concluded that facies similarities such as *Renalcis* mound and flaser-bedded intertidal ribbon rock reflect anomalous oceanic conditions resulting in low biodiversity and low intensity of bioturbation after the end-Permian extinction. Similarities in cycle stacking patterns reflect low-amplitude, high-frequency sea-level fluctuations resulting from greenhouse conditions common to the Early Paleozoic and Early Triassic.

The three-order hierarchical stratigraphic relationship as suggested by Lehrmann *et al.* (2001) was quantitatively tested by Yang and Lehrmann (2003) through time series and spectral analysis of cycle thickness and facies data of DJ and DW sections (Figure 4). Milankovitch climatic signals of prominent short-eccentricity (94.9−131.2 kyr), short-obliquity (35.8 kyr), and long precessional index (21.2 kyr), and minor long-eccentricity (412.9 kyr), long-obliquity (45.3 kyr), short precessional index (17.7 kyr), and a constructional-tone (9.7 kyr) were detected. The estimated stratigraphic completeness is much greater than that of icehouse stratigraphic records. The results suggest that Milankovitch climatic forcing had greatly influenced sedimentation. Yang and Lehrmann (2003) speculated that variations in carbonate productivity and environmental conditions driven by Milankovitch climatic forcing, combined with low-amplitude sea-level fluctuations, were likely major controls on cyclic sedimentation. Furthermore, evolutive spectra of the two sections show that dominant Milankovitch climatic forcings varied from short eccentricity, obliquity, to long-precessional index during the course of sedimentation, suggesting variations in the type and magnitude of oceanic and climatic processes and their mechanisms during the course of cyclic sedimentation of DJ and DW sections. Finally, the DW and DJ cycles accumulated during the Early Triassic aftermath of end-Permian mass extinction. This period is characterized by extremely low biodiversity, a mollusk-dominated skeletal biota, low skeletal abundance, extremely small and lightly calcified fauna (*e.g.*, Payne *et al.*, 2006), and microbial and cement precipitates (*e.g.*, Woods *et al.*, 1999; Lehrmann *et al.*, 2003; Payne *et al.*,

2007). A decimated carbonate productivity potential and detrimental environmental conditions (*e.g.*, anoxia and euxinia) had been the norm during the delayed recovery from the extinction (*e.g.*, Payne *et al.*, 2004). The lithologic and stratigraphic characteristics and the controlling processes and mechanisms of the DW and DJ cyclicity can be better understood in this global and temporal context as discussed below.

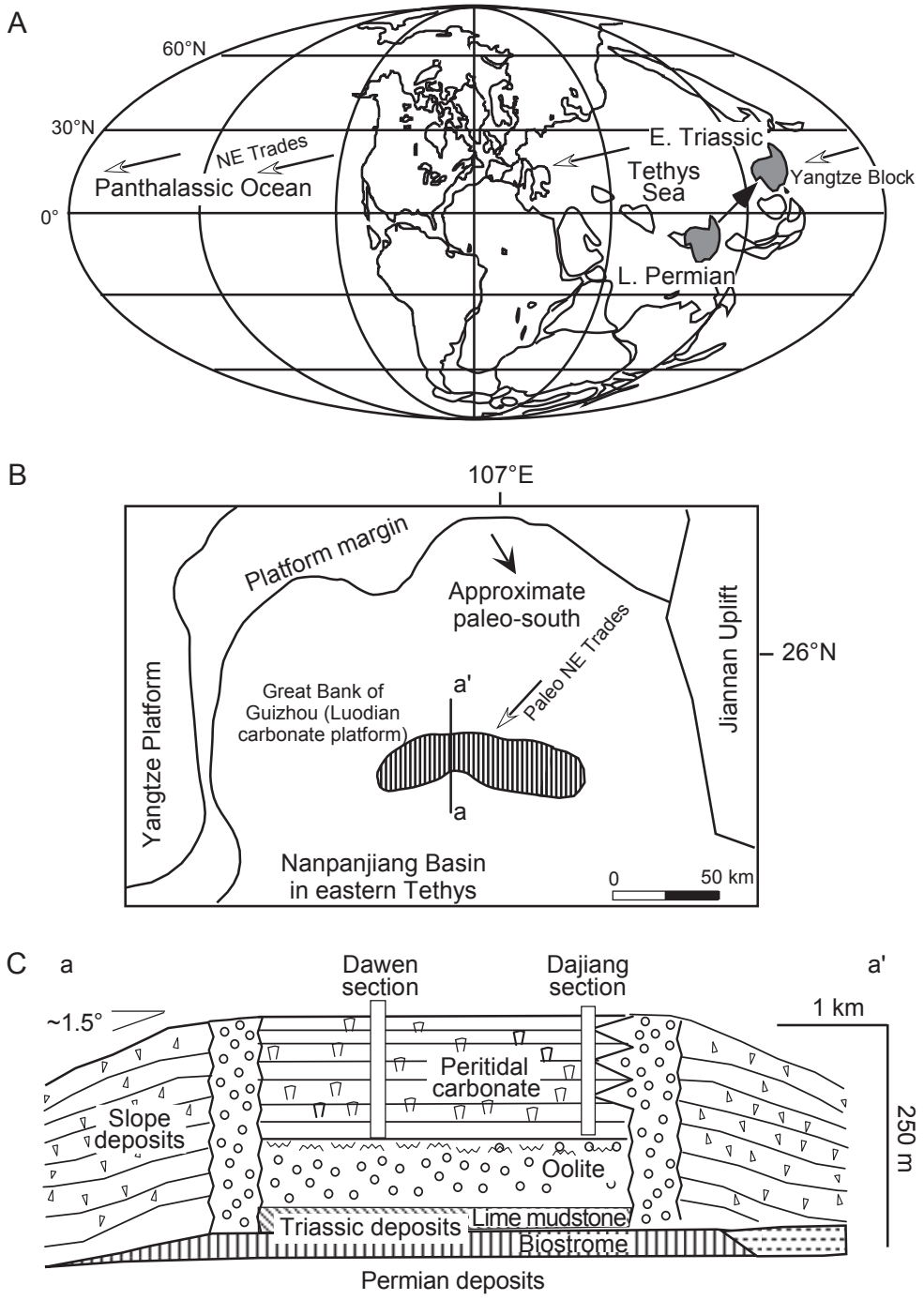

Figure 1 A−Paleogeographic location of Yangtze Block at ~12°N latitude, which migrated across the paleoequator from the end of Permian to the Early Triassic. Modified from Scotese (1994); B−Early Triassic paleogeography of Nanpanjiang Basin compiled from regional geologic maps by Bureau of Geology and Mineral Exploration and Development of Guizhou Province (1987) and Bureau of Geology and Mineral Resources of Guangxi Zhuang Autonomous Region (1985), showing location of the Great Bank of Guizhou or Luodian Carbonate Platform; C−Restored Lower Triassic cross-section of the bank, showing stratigraphic architecture and location of Dawen and Dajiang sections. See B for location. After Lehrmann *et al.*, 2001.

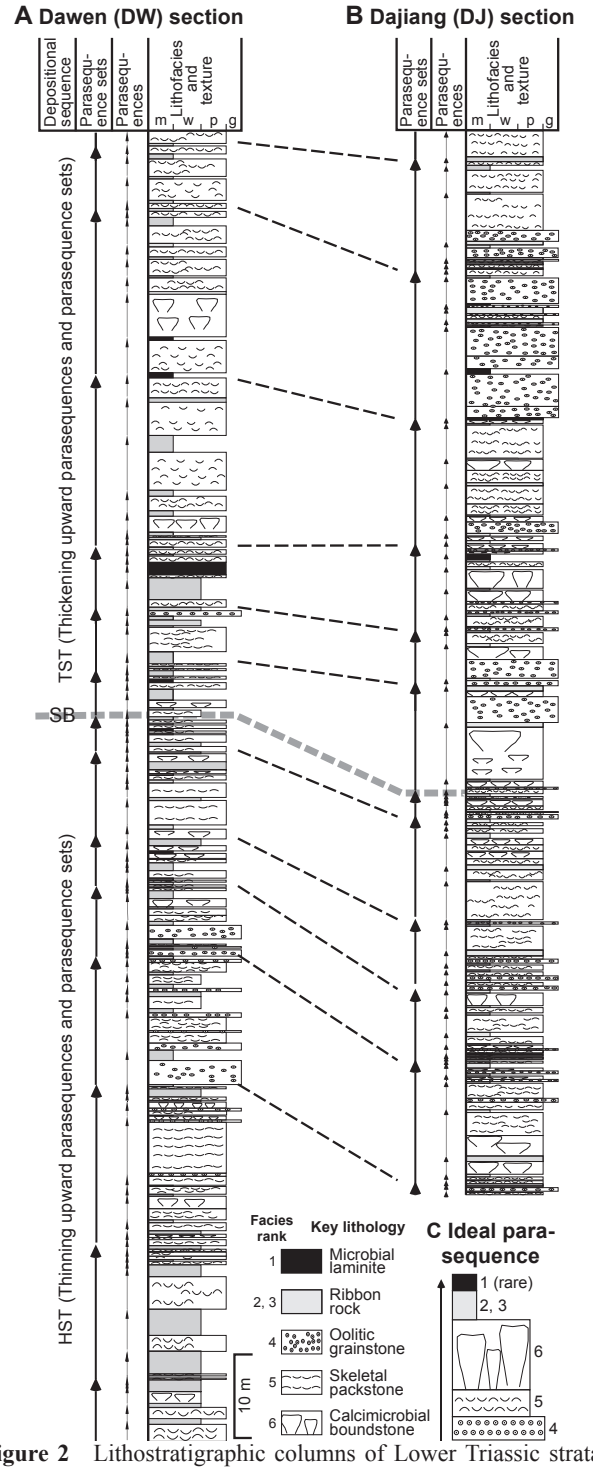

Figure 2 Lithostratigraphic columns of Lower Triassic strata in Dawen (A) and Dajiang (B) sections. Three orders of cycles, namely parasequences, parasequence sets, and depositional sequences, were identified. Systems tracts and sequence boundary of depositional sequences are indicated. TST = transgressive systems tract; HST = highstand systems tract; SB = sequence boundary; m = mudstone; w = wackestone; p = packstone; g = grainstone; dashed line indicates tentative correlation. The typical or "ideal" parasequence is shown in C. Modified from Lehrmann *et al.*, 2001. Facies ranks interpret relative water depth of component lithofacies.

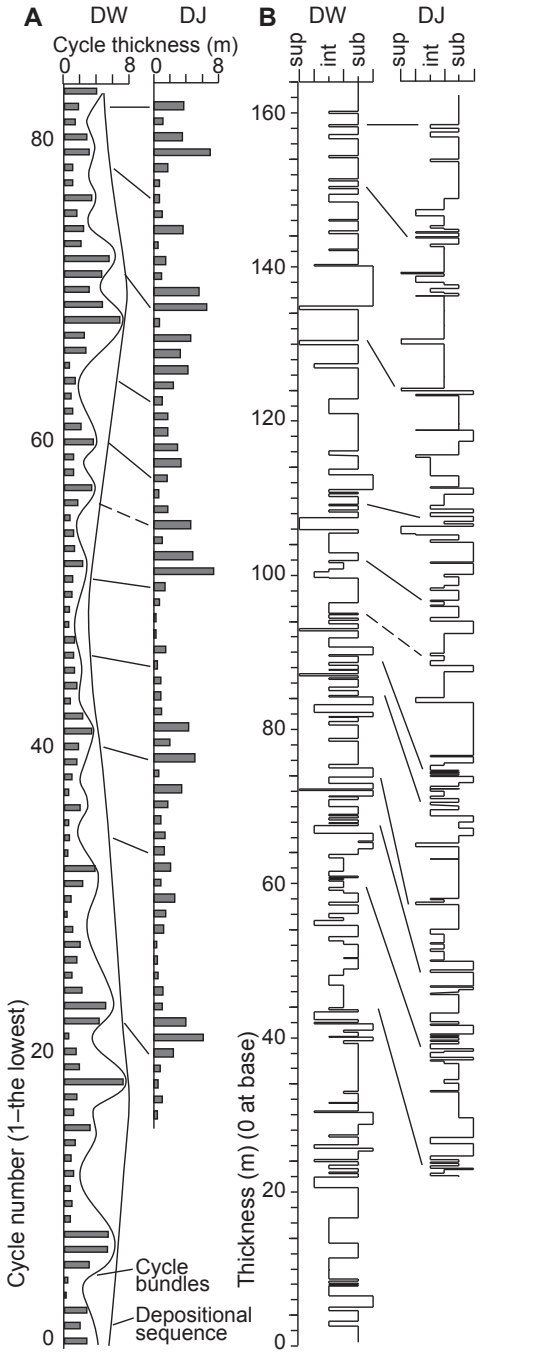

Figure 3 Variations in thickness (A) and component facies (B) of the Dawen (DW) and Dajiang (DJ) sections (Figure 1C). The average and range of cycle thickness are 2.0 m and 0.2−7.1 m for DW and 2.1 m and 0.25−7.4 m for DJ. Left panel: Cycle thickness pattern of cycle bundles in a depositional sequence of the DW section shows a three-order hierarchy and is correlative to the DJ section (Lehrmann *et al.*, 2001). Right panel: Subtidal and intertidal facies dominate, with rare supratidal facies in the upper part of the sections. The facies curves were used in spectral analysis of Yang and Lehrmann (2003). Lines between two sections are correlation lines, dashed where it is tentative. "sub", "int", and "sup" represent subtidal, intertidal, and supratidal facies, respectively.

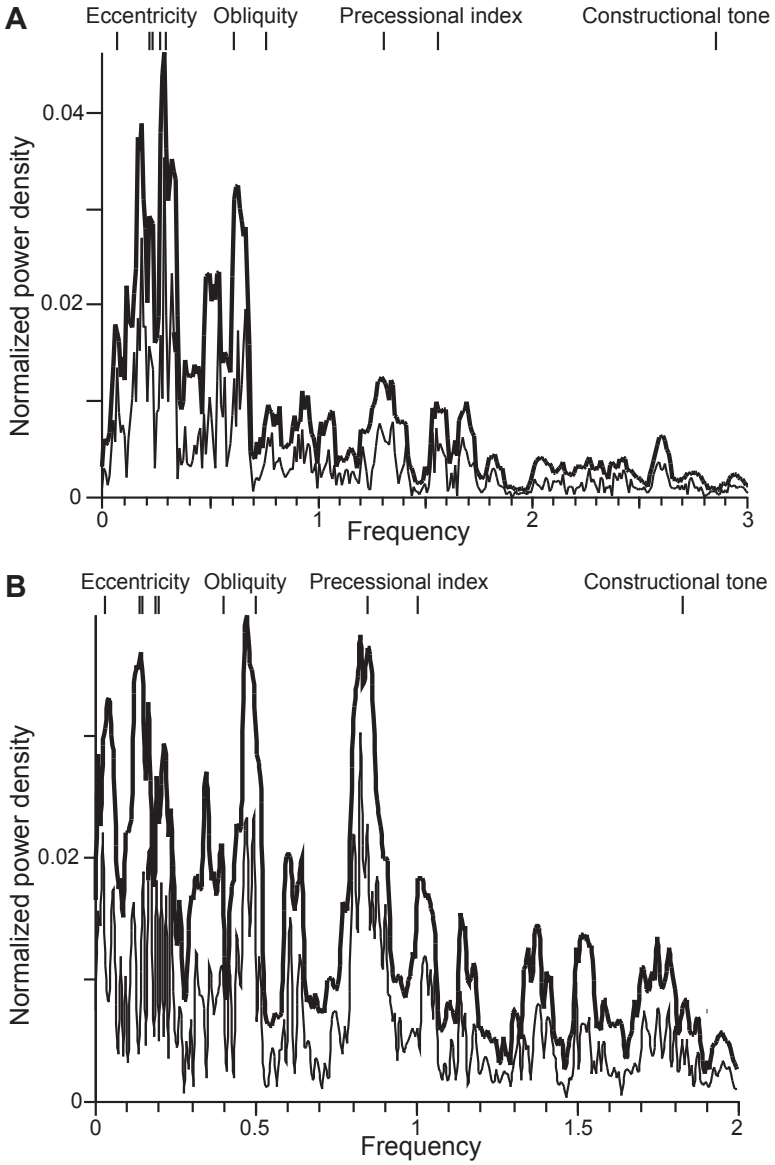

Figure 4 Spectra of Dajiang (A) and Dawen (B) sections time series. Thick lines are spectra; thin lines below the spectral lines are lower than 90% confidence limits; thin vertical lines above the spectral lines are Milankovitch line spectra at 247 Ma (Berger *et al.*, 1992). Nyquist frequency is 25 for Dajiang and 20 for Dawen spectra. Thickness-time conversion, spectral analysis, and period calibration were conducted separately for the two sections. See Yang and Lehrmann (2003) for details. The calibrated spectra contain prominent short-eccentricity, short-obliquity, and long-precession index peaks, and minor long-eccentricity, long-obliquity, short-precession index, and constructional-tone peaks. Thus, Milankovitch climatic forcing probably greatly influenced cyclic sedimentation of DJ and DW sections.

3 Carbonate productivity variations

Intra- and inter-cycle variations in carbonate productivity are interpreted from facies type, thickness, stacking pattern, and estimated sedimentation rate of DJ and DW cycles. Intertidal and supratidal sediments are mainly transported from the subtidal factory and redistributed on the tidal flat. Large subtidal production will likely generate copious sediments to quickly fill the accommodation space, resulting in shallowing-upward subtidal−intertidal−supratidal successions, whereas small production results in thin intertidal and supratidal facies or absence of these facies, assuming the rate of accommodation space generation is constant. Sea-level change was minimal during the Early Triassic because of the absence of continental glaciers; and the subsidence of the platform was approximately constant at a cycle scale. Thus, the rate of accom-

modation space generation on the bank was relatively constant. As a result, facies type and thickness of DJ and DW cycles are first-order indicators of carbonate productivity, even though sediment redistribution and preservation may affect facies type and thickness.

Several lines of evidence from the DJ and DW cycles provide clues on benthic carbonate productivity and its intra-cycle variations. First, the low-diversity biota of cyanobacteria, echinoderms, bivalves, gastropods, lingulid brachiopods, spirorbids, and ostracodes, and the low abundance of skeletal grains (Payne *et al.*, 2006) suggest low carbonate productivity. Ooid production in the marginal shoals was high enough to export ooids to the interior (Figures 1C, 2; Lehrmann *et al.*, 2001). However, oolitic facies are thin and uncommon (0.9 m thick on average; 14% in total thickness), suggesting that chemical precipitates were subordinate to skeletal and mound sediments, which are 1.3 m thick on average. Second, the effective accumulation rate of subtidal facies is 31−24 cm/ky, an order of magnitude higher than that (6−3 cm/ky) of combined intertidal and supratidal facies, as estimated by Yang and Lehrmann (2003) on the basis of Milankovitch cycle period calibration. The rates indicate decreased productivity during intertidal and supratidal deposition (Figure 5).

Third, the intertidal facies is thin, 0.5 m thick on average (Figure 3). The supratidal facies is not only thin, 0.7 m thick on average, but also rare, only presents in 14 out of 149 cycles. These facts indicate common termination of intertidal deposition before the available intertidal and supratidal space was filled. The termination may have four causes: subaerial exposure due to a sea-level fall, drowning by a sea-level rise, some unknown random processes, or a productivity shutdown due to environmental stress (Tucker *et al.*, 1990; Schlager, 2005). Thick intertidal and supratidal facies commonly occur during tidal flat progradation accompanying a sea-level fall. Thus, the thin intertidal facies and rare supratidal facies suggest that a sea-level fall during intertidal and supratidal deposition likely did not occur. The fall, if it occurred, was likely short and minimal, as indicated by the absence of prolonged subaerial exposure on subtidal facies. A small sea-level rise is also not likely, because it will not be able to drown the platform; on the contrary, it may increase carbonate productivity in the interior (Schlager, 2005). Any random processes, such as episodic subsidence, will not generate cycle hierarchy. Thus, a drastic reduction of sediment productivity in the subtidal factory caused by environmental stresses during intertidal deposition is the only plausible mechanism causing the termination of intertidal deposition and rarity of supratidal facies.

Inter-cycle variations in cycle and facies thickness and facies type indicate long-term environmental and productivity changes (Figures 2, 3; cf. Drummond and Wilkinson, 1993b; Lehrmann *et al.*, 1998, 2001; Yang and Lehrmann, 2003). The occurrence of supratidal facies in the middle and upper DW and DJ sections, although rare, coincides with limited taxonomic recovery and, perhaps, pulses of increased productivity during the Induan (*e.g.*, Kozur, 1998; Twitchett *et al.*, 2004; Chen *et al.*, 2007). There are also systematic upsection changes in the proportions of ooids, calcimicrobial mud, and skeletal grains. The evolving Milankovitch signal upsection correlates with changes in cycle thickness and facies type. For example, in DW section, the 0−60 m segment contains a mixture of thick to moderately thick cycles (Figures 2, 3); and some of the thick cycles are probably bundles of thin cycles. This is reflected in a dominant eccentricity signal in the evolutive Milankovitch spectrum (see Yang and Lehrmann, 2003, for evolutive spectra of DJ and DW sections). The 40−80 m segment contains predominantly thin cycles of approximately equal thickness and abundant oolites. This is reflected in a dominant obliquity signal. The occurrence of both thick and very thin cycles in the 100−140 m segment is reflected by co-existing precessional index and short-eccentricity signals. The occurrence of thin but approximately equal thickness cycles in the 120−160 m segment is reflected by the dominant precessional index and a minor constructional tone signal (Figures 2, 3; Yang and Lehrmann, 2003). Finally, the 60−100 m segment in the middle DW section contains mixed thin and moderately thick cycles and covers the stratigraphic turning point from the upper highstand systems tract to the lower transgressive systems tract across a sequence boundary (Figures 2, 3). The spectrum of this segment has a broad peak centered on the obliquity band, probably as a result of mixing of obliquity in the lower part and precessional index in the upper part.

The above discussions on intra- and inter-cycle variations of facies type and cycle and facies thickness, as well as their correlation with Milankovitch climatic forcings, suggest a cause-effect relationship between Milankovitch climatic forcing and multi-order cyclic sedimentation in a greenhouse climate in an equatorial mid-ocean setting. However, the oceanographic and sedimentary mechanisms that link climatic forcings with stratigraphic characteristics of DW and DJ cycles are not clear (Yang and Lehrmann, 2003). For example, orbital eccentricity and obliquity are physically independent, whereas the precessional index is

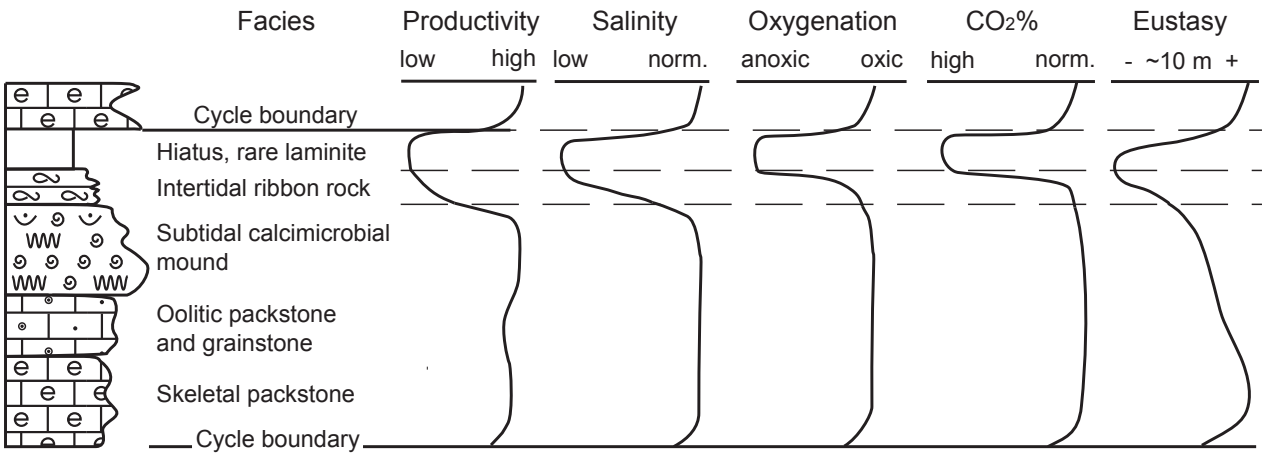

Figure 5 Speculations on temporal variations of facies and relationships among subtidal sediment productivity, environmental factors, and eustasy during the deposition of an ideal Dawen and Dajiang cycle. Environmental perturbations in the subtidal zone may be the main cause of intra-cycle productivity variations in a greenhouse climate when eustasy was minimal, as indicated by the common termination of intertidal deposition, rarity of supratidal facies, and lack of prolonged subaerial exposure in those cycles.

modulated by the eccentricity (Berger, 1977, 1988; Berger *et al.*, 1992; cf. Liu *et al.*, 2000) and, thus, the climatic forcings affected and interacted with geologic processes nonlinearly (*e.g.*, Ripepe and Fischer, 1991; deMenocal, 1995). Formation, distribution, and deposition of oolitic sediments are closely related to climatic and oceanic conditions that affect the energy and water chemistry of the windward platform margin. The frequency and strength of tropical storms would affect the extent and thickness of oolite spill-over lobes into the platform interior (Figure 1C). Plate reconstructions place the study area at 12°N latitude facing N45°E into the northeast trade winds (Figure 1; Kutzbach *et al.*, 1990; Crowley, 1994; Scotese, 1994; Scotese *et al.*, 1999). Thus, obliquity forcing may have been transferred to the sedimentary record via equatorial atmospheric circulation (cf. Crowley, 1994).

Furthermore, the upsection spectral shift in Milankovitch climatic forcings in the DW and DJ records suggests that no one mechanism dominated through the entire course of sedimentation. If the evolving Milankovitch signals were mainly caused by an estimated 6°−7° northward plate movement during the Olenekian, the latitudinal climatic gradient in the eastern Tethys must have been very steep, conforming with a similar interpretation from the low-latitude continental record in Late Triassic western Pangea (Kent and Olsen, 2000). The other possible scenario is that, assuming the amount of plate movement is insignificant during the Olenekian, the evolving Milankovitch climatic forcing may have been caused mainly by dynamic changes of global atmospheric and oceanic conditions. Temporal changes of dominant Milankovitch climatic forcing at a given locality were documented in continental northwestern Africa in the Plio-Pleistocene (*e.g.*, deMenocal, 1995), and should have been common in geological records (Berger, 1988; see Hinnov and Park, 1998; Meyers *et al.*, 2001; Pälike *et al.*, 2001 for more examples) because of the complex interaction of atmospheric and oceanic systems (*e.g.*, Crowley, 1994). The above speculations on paleoclimatic and oceanographic changes suggest that sedimentary processes and mechanisms other than sea-level fluctuations may have played a major role in cyclic sedimentation in the study area. Some specific mechanisms are speculated in the following sections.

4 Factors controlling carbonate productivity variations

Factors affecting subtidal carbonate productivity on the Great Bank of Guizhou include salinity, possible incursions of toxic anoxic and euxinic waters, nutrient levels, and water depth. Each factor is considered separately below.

First, the slowly-recovering biota was sensitive to salinity variations of the bank water (Figure 5). Salinity changes due to varying evaporation that was induced by sea-surface temperature changes were likely minimal, because temperature varied little in the low-latitude ocean and equable greenhouse climate (Kutzbach, 1994). However, hyposalinity prevailed in the bank interior during periods of high rainfall of the megamonsoonal climate over

the Tethys (Kutzbach and Gallimore, 1989; Parrish, 1993; Crowley, 1994). Rainfall may have varied 33% in the low-latitude east coast in a precession cycle (Kutzbach, 1994); and peak temperature on land correlated with maximum rainfall and hyposalinity in coastal regions due to precessional forcing modulated by 100 ky cycles in the Early Triassic (Crowley, 1994). Varying monsoon intensity at the precessional and eccentrical scales would have caused rainfall and, thus, intra-cycle salinity variations. Hence, intertidal deposition occurred during periods of low rainfall and high carbonate productivity, followed by nondeposition during periods of high rainfall and low productivity. In addition, the greater proportion of supratidal facies in the upper sections (Figures 2, 3) indicates an increase in carbonate production, probably related to a long-term reduction of monsoon intensity, more saline marine water, and enhanced carbonate productivity in response to northward migration of the South China Plate across the equator to ~15°N from 240−250 Ma (Kutzbach, 1994; Scotese, 1994).

Second, toxic deep anoxic waters, also loaded with CO_2 and H_2S, may have poisoned the benthos. Although the causes of the end-Permian extinction are still debatable, there is general agreement that deep oceanic waters were anoxic and likely also euxinic and charged with CO_2 throughout the Early Triassic (Hallam, 1991; Schubert and Bottjer, 1995; Knoll *et al.*, 1996; Wignall and Hallam, 1996; Wignall and Twitchett, 1996; Isozaki, 1997; Heydari *et al.*, 2000; Payne *et al.*, 2004; Kump *et al.*, 2005; Meyer *et al.*, 2008). Meyer and Kump′s (2008) results of Earth system modeling support a link between oceanic nutrient status and the redox state of the end-Permian ocean. Modest increases in marine phosphate concentration can result in widespread deep ocean euxinia. Hydrogen sulfide built up in the Paleo-Tethys Ocean relative to the Panthalassic Ocean due to nutrient-trapping ocean circulation in the Paleo-Tethys. These toxic bottom waters, when delivered to the banktop, would have decimated benthic biota and drastically reduced benthic carbonate productivity and sediment production.

The delivery mechanisms include rising of the toxic waters in the water column via upwelling, mixing and/or overturn of deep to surface water masses, and small fluctuations of sea level causing toxic floodings. Recent modeling of Meyer and Kump (2008) and Meyer *et al.* (2008) suggested that upwelling delivered deep sulfidic waters to the photic zone in the eastern Paleo-Tethys in Guizhou and the preferential buildup of nutrients in the restricted Tethys greatly exacerbated euxinia in the region. In addition, mixing may have occurred due to intensified oceanic upwelling and downwelling caused by, for example, global seasonality variations and increased equator-to-pole temperature gradient related to the obliquity forcing (Kutzbach and Gallimore, 1989; Kutzbach *et al.*, 1990; Kutzbach, 1994; Wignall and Twitchett, 1996; Parrish *et al.*, 2001). Wignall and Twitchett (1996) documented anoxic flooding above storm wavebase (see also Kozur, 1998) and fluctuations of anoxic, dysaerobic, and oxic conditions on the Early Triassic platforms in western Tethys. Similarly, seafloor aragonite fans suggest upwelling of anoxic, alkaline waters in the Early Triassic shelf and slope of the western Pangea (Woods *et al.*, 1999).

The study area in the low-latitude eastern Tethys was prone to toxic water flooding onto the shelf where strong ocean currents were common (Kutzbach *et al.*, 1990). Repeated incursions of toxic water masses over the banktop were facilitated by transgressions during or shortly after intertidal deposition and caused termination of intertidal deposition and absence of supratidal facies, or even entire intertidal facies in 11 of a total 149 DW and DJ cycles (Figure 5). After termination, subtidal deposition gradually resumed in the space created by continued subsidence and, possibly, a sea-level rise. As a result, the subtidal facies overlie the intertidal facies without a prominent exposure surface. The rarity of supratidal facies, lack of prominent subaerial exposure surfaces, and correlative cycles of DW and DJ sections (Figures 2, 3; Lehrmann *et al.*, 2001) support this interpretation that banktop flooding of toxic waters poisoned the benthic biota, causing a great reduction in carbonate productivity. Finally, the varying precessional and obliquitous signals on the DW and DJ evolutive spectra (Yang and Lehrmann, 2003) suggest alternating sluggish and active oceanic circulation, which would have induced hierarchical variations of carbonate productivity at the Milankovitch cycle scale.

Third, excessive nutrients in the water (*e.g.*, Meyer and Kump, 2008) will suffocate benthos to reduce carbonate productivity (Figure 5; Hallock and Schlager, 1986). The superanoxia of Early Triassic oceans (*e.g.*, Isozaki, 1997) also suggests a high overall primary productivity in Panthalassa. But the DW and DJ rocks are not enriched in organic matter and phosphate (cf. Woods *et al.*, 1999; Parrish *et al.*, 2001). However, the recurring growth of calcified microbialite in these cycles was likely stimulated by pulses of increased nutrients (cf. Lehrmann, 1999; Lehrmann *et al.*, 2001). Further geochemical work is needed to evaluate the possibility of excess nutrients and potential linkage with upwelling. If there were significant pulses of excess

nutrients to the banktop, cycling of organic matter or other factors may have inhibited organic matter preservation in the sediment.

Last, eustasy may have changed the water depth and, thus, the subtidal productivity on the platform (Figure 5; *e.g.*, Pittet *et al.*, 2000). Shoaling, subsidence, and non-glacial eustasy (Kutzbach, 1994; Scotese *et al.*, 1999) all affect water depth. Non-glacial eustasy of several to a few tens of meters (*e.g.*, Cisne and Gildner, 1988) can be driven by Milankovitch forcing via changing continental water storage (Jacobs and Sahagian, 1993), the Earth′s internal responses to orbital variations (Mörner, 1994), and thermal ocean expansion (Schulz and Schäfer-Neth, 1997; see also Pindell and Drake, 1998). Eustasy affected accommodation space and, thus, the cycle thickness. But the rare supratidal facies and vadose meteoric alteration, and the lack of prominent subaerial exposure surfaces directly on subtidal facies indicate a minimal effect. A small sea-level rise will deepen the subtidal zone and slightly increase carbonate productivity. More likely, the rise would aid the platform with flooding of anoxic and/or CO_2-charged deep water.

5 Productivity-driven cyclic peritidal carbonate sedimentation

We propose a conceptual model that explains how temporal variations in carbonate productivity alone can form

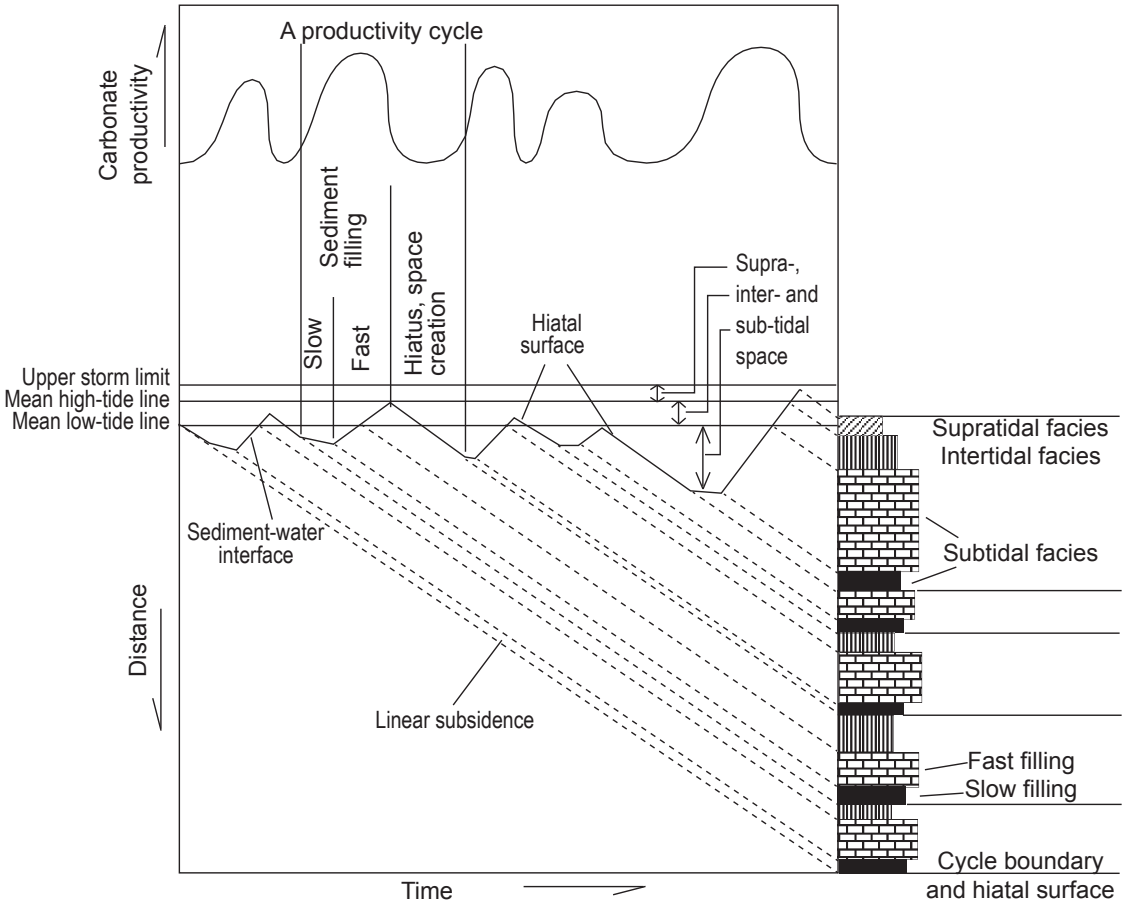

Figure 6 A one-dimensional conceptual model of peritidal cyclic sedimentation under constant sea level and subsidence, and fluctuating carbonate productivity. The productivity variations in the subtidal zone are ordered and mainly caused by environmental perturbations induced by Milankovitch climatic and oceanographic processes. During minimal productivity, deposition on the tidal flat ceases, terminating intertidal or even subtidal deposition to form a nondepositional hiatus; in the meanwhile, subsidence is creating more depositional space. During a gradual productivity increase, the space is slowly filled to form the lower subtidal facies. During peak productivity, sediments fill the subtidal and intertidal space. The subtidal space is only partially filled if the peak production is low; the supratidal space is filled if the peak is high. During a sharp productivity decline, sediment accumulation is minimal. This model shows that meter-scale peritidal carbonate cycles can be formed by productivity variations alone. Adding small sea-level fluctuations (not shown) will accentuate depositional space variations without affecting the general stratigraphic pattern.

shallowing-upward peritidal cycles under constant subsidence and sea level (Figure 6). The productivity varies in four phases from non-productive, gradual increase, peak, to rapid decline; and a lag time is included in the non-productive phase (cf. Read *et al.*, 1986). If subtidal carbonate productivity is proportional to production of carbonate sediments, the model produces shallowing-upward cycles dominated by subtidal and intertidal facies, and cycles containing only subtidal facies or subtidal-supratidal facies when productivity is extremely low or high, respectively (Figure 6). Adding small sea-level changes in the model slightly changes depositional space without altering the overall stratigraphic pattern. Lateral variations in accommodation space, productivity, and sediment redistribution on the platform (*e.g.*, Pratt and James, 1986; Osleger, 1991) related to topography and type of benthos will also cause autogenic variations in the type, timing, and amount of sediment accumulation. The stratigraphic hierarchy of the DW and DJ successions, however, suggests these variations are secondary. The conceptual model shows how subtidal carbonate productivity variations induced by Milankovitch-related climatic and oceanographic processes may have formed the hierarchical facies and thickness patterns of DW and DJ cycles.

The productivity-driven succession has a high stratigraphic completeness. Yang and Lehrmann (2003) estimated a 36%−75% and 47%−98% completeness for DW and DJ sections, respectively, which is high in comparison to 10%−20% for Phanerozoic peritidal carbonate cycles (Sadler, 1994) and 3%−30% for Paleozoic peritidal carbonate cycles (Wilkinson *et al.*, 1991; Yang *et al.*, 1995). The high completeness is attributed to the small eustasy and may be characteristic of productivity-driven greenhouse peritidal cycles.

This model demonstrates that the formation of greenhouse carbonate cycles (*e.g.*, Goldhammer *et al.*, 1990; Zempolich, 1993; among many others) may not require eustasy of several tens of meters. The autocyclic model of Goldhammer *et al.* (1990) assumed no 4th and 5th-order eustasy but constant subtidal sedimentation regulated by lag depth, which, in fact, causes productivity variations by shutting down the subtidal carbonate factory when the platform was within the lag depth. The biota in the study area was particularly vulnerable to environmental perturbations. The cyclicity observed in other carbonate platforms may also reflect primary influence of fluctuating carbonate productivity. However, in cases of a robust biota that can produce copious sediments to quickly fill the accommodation space, peritidal sedimentation would be mainly controlled by eustasy. In all cases, productivity variations always exist and should be considered in interpreting cyclic carbonate sedimentation.

Acknowledgements

We thank S. Mazzullo, K. Meyer, E. Rankey, B. Wilkinson, and Mei-Yi Yu for discussions, and the late R. Goldhammer, D. Bosence, P. Burgess, D. Pollit, E. Rankey, W. Schlager, and N. Tabor for insightful reviews of the early drafts. We appreciate the constructive comments from Journal of Palaeogeography reviewers Professor Ming-Xiang Mei and Professor Zeng-Zhao Feng, which improved the quality of the paper.

References

Berger, A., 1977. Support for the astronomical theory of climatic change. Nature, 269(5623): 44−45.

Berger, A., 1988. Milankovitch theory and climate. Reviews of Geophysics, 26(4): 624−657.

Berger, A., Loutre, M. F., Laskar, J., 1992. Stability of the astronomical frequencies over the Earth′s history for paleoclimate studies. Science, 255(5044): 560−566.

Bureau of Geology and Mineral Exploration and Development of Guizhou Province, 1987. Regional Geology of Guizhou Province. Beijing: Geological Publishing House, 1−698 (in Chinese with English contents and brief text; geologic map scale 1:500, 000).

Bureau of Geology and Mineral Resources of Guangxi Zhuang Autonomous Region, 1985. Regional Geology of Guangxi Zhuang Autonomous Region, People′s Republic of China. Beijing: Geological Publishing House, 1−853 (in Chinese with English contents and brief text; geologic map scale 1:500,000).

Burgess, P. M., 2001. Modeling carbonate sequence development without relative sea-level oscillations. Geology, 29(12): 1127−1130.

Burgess, P. M., 2008. The nature of shallow-water carbonate lithofacies thickness distributions. Geology, 36(3): 235−238.

Chen, Z. Q., Tong, J. N., Kaiho, K., Kawahata, H., 2007. Onset of biotic and environmental recovery from the end-Permian mass extinction within 1−2 million years: A case study of the Lower Triassic of the Meishan Section, South China. Palaeogeography, Palaeoclimatology, Palaeoecology, 252(1−2): 176−187.

Cisne, J. L., Gildner, R. F., 1988. Measurement of sea-level change in epeiric seas: The Middle Ordovician transgression in the North American midcontinent. In: Wilgus, C. K., Hastings, B. S., Kendall, C. G. St. C., Posamentier, H., Ross, C. A., van Wagoner, J. C., (eds). Sea-Level Changes: An Integrated Approach. SEPM Special Publications, 42: 183−213.

Crowley, T. J., 1994. Pangean climates. In: Klein, G. D., (ed). Pangea: Paleoclimate, Tectonics, and Sedimentation during Ac-

cretion, Zenith and Breakup of a Supercontinent. GSA Special Papers, 288: 25−40.

deMenocal, P. B., 1995. Plio-Pleistocene African climate. Science, 270(5233): 53−59.

Drummond, C. N., Wilkinson, B. H., 1993a. Aperiodic accumulation of cyclic peritidal carbonate. Geology, 21(11): 1023−1026.

Drummond, C. N., Wilkinson, B. H., 1993b. On the use of cycle thickness diagrams as records of long-term sealevel change during accumulation of carbonate sequences. Journal of Geology, 101(6): 687−702.

Feng, Z. Z., Bao, Z. D., Li, S. W., 1997. Lithofacies Palaeogeography of Early and Middle Triassic of South China. Beijing: Petroleum Industry Press, 1−222, photoplates 1−26, colour maps 1−4 (in Chinese with English preface, contents and abstracts).

Frakes, L. A., Francis, J. E., Syktus, J. I., 1992. Climate Modes of the Phanerozoic. Cambridge: Cambridge University Press, 1−274.

Ginsburg, R. N., 1971. Landward movement of carbonate mud: New model for regressive cycles in carbonates (abstract). AAPG Bulletin, 55(2): 340.

Goldhammer, R. K., Dunn, P. A., Hardie, L. A., 1990. Depositional cycles, composite sea-level changes, cycle stacking patterns, and the hierarchy of stratigraphic forcing: Examples from Alpine Triassic platform carbonates. GSA Bulletin, 102(5): 535−562.

Hallam, A., 1991. Why was there a delayed radiation after the end-Paleozoic mass extinctions? Historical Biology, 5(2−4): 257−262.

Hallock, P., Schlager, W., 1986. Nutrient excess and the demise of coral reefs and carbonate platforms. Palaios, 1(4): 389−398.

Heydari, E., Hassandzadeh, J., Wade, W. J., 2000. Geochemistry of central Tethyan Upper Permian and Lower Triassic strata, Abadeh region, Iran. Sedimentary Geology, 137(1−2): 85−99.

Hinnov, L. A., Park, J., 1998. Detection of astronomical cycles in the stratigraphic record by frequency modulation (FM) analysis. Journal of Sedimentary Research, 68(4): 524−539.

Isozaki, Y., 1997. Permo-Triassic boundary superanoxia and stratified superocean: Records from the lost deep sea. Science, 276(5310): 235−238.

Jacobs, D. K., Sahagian, D. L., 1993. Climate-induced fluctuations in sea level during non-glacial times. Nature, 361(6414): 710−712.

Kent, D. V., Olsen, P. E., 2000. Magnetic polarity stratigraphy and paleolatitude of the Triassic−Jurassic Blomidon Formation in the Fundy Basin (Canada): Implications for Early Mesozoic tropical climate gradients. Earth and Planetary Science Letters, 179(2): 311−324.

Knoll, A. H., Bambach, R. K., Canfield, D. E., Grotzinger, J. P., 1996. Comparative Earth history and the Late Permian mass extinction. Science, 273(5274): 452−457.

Kozur, H. W., 1998. Some aspects of the Permian−Triassic boundary (PTB) and of the possible causes for the biotic crisis around this boundary. Palaeogeography, Palaeoclimatology, Palaeoecology, 143(4): 227−272.

Kump, L. R., Pavlov, A., Arthur, M. A., 2005. Massive release of hydrogen sulfide to the surface ocean and atmosphere during intervals of oceanic anoxia. Geology, 33(5): 397−400.

Kutzbach, J. E., 1994. Idealized Pangean climates: Sensitivity to orbital changes. In: Klein, G. D., (ed). Pangea: Paleoclimate, Tectonics, and Sedimentation during Accretion, Zenith and Breakup of a Supercontinent. GSA Special Papers, 288: 41−56.

Kutzbach, J. E., Gallimore, R. G., 1989. Pangaean climates: Megamonsoons of the megacontinent. Journal of Geophysical Research: Atmospheres, 94(D3): 3341−3357.

Kutzbach, J. E., Guetter, P. J., Washington, W. M., 1990. Simulated circulation of an idealized ocean for Pangaean time. Paleoceanography, 5(3): 299−317.

Lehrmann, D. J., 1993. The Great Bank of Guizhou: Birth, evolution and death of an isolated Triassic carbonate platform, Guizhou Province, South China [Ph. D. thesis]. Lawrence: University of Kansas, 1−457.

Lehrmann, D. J., 1999. Early Triassic calcimicrobial mounds and biostromes of the Nanpanjiang basin, south China. Geology, 27(4): 359−362.

Lehrmann, D. J., Payne, J. L., Felix, S. V., Dillett, P. M., Wang, H. M., Yu, Y. Y., Wei, J. Y., 2003. Permian−Triassic boundary sections from shallow-marine carbonate platforms of the Nanpanjiang Basin, South China: Implications for oceanic conditions associated with the end-Permian extinction and its aftermath. Palaios, 18(2): 138−152.

Lehrmann, D. J., Wei, J. Y., Enos, P., 1998. Controls on facies architecture of a large Triassic carbonate platform: The Great Bank of Guizhou, Nanpanjiang Basin, South China. Journal of Sedimentary Research, 68(2): 311−326.

Lehrmann, D. J., Yang, W., Wei, J. Y., Yu, Y. Y., Xiao, J. F., 2001. Lower Triassic peritidal cyclic limestone: An example of anachronistic carbonate facies from the Great Bank of Guizhou, Nanpanjiang Basin, Guizhou Province, South China. Palaeogeography, Palaeoclimatology, Palaeoecology, 173(3−4): 103−123.

Liu, Z. Y., Kutzbach, J., Wu, L. X., 2000. Modeling climate shift of El Nino variability in the Holocene. Geophysical Research Letters, 27(15): 2265−2268.

Meyer, K. M., Kump, L. R., 2008. Oceanic euxinia in Earth history: Causes and consequences. Annual Review of Earth and Planetary Sciences, 36: 251−288.

Meyer, K. M., Kump, L. R., Ridgwell, A., 2008. Biogeochemical controls on photic-zone euxinia during the end-Permian mass extinction. Geology, 36(9): 747−750.

Meyers, S. R., Sageman, B. B., Hinnov, L. A., 2001. Integrated quantitative stratigraphy of the Cenomanian−Turonian Bridge Creek Limestone Member using evolutive harmonic analysis and stratigraphic modeling. Journal of Sedimentary Research, 71(4): 628−644.

Mörner, N. A., 1994. Internal response to orbital forcing and external cyclic sedimentary sequences. In: de Boer, P. L., Smith, D. G., (eds). Orbital Forcing and Cyclic Sequences. IAS Special Publications, 19: 25−33.

Osleger, D., 1991. Subtidal carbonate cycles: Implications for allocyclic vs. autocyclic controls. Geology, 19(9): 917−920.

Pälike, H., Shackleton, N. J., Röhl, U., 2001. Astronomical forcing

in Late Eocene marine sediments. Earth and Planetary Science Letters, 193(3−4): 589−602.

Parrish, J. T., 1993. Climate of the supercontinent Pangea. Journal of Geology, 101(2): 215−233.

Parrish, J. T., Droser, M. L., Bottjer, D. J., 2001. A Triassic upwelling zone: The Shublik Formation, Arctic Alaska, U.S.A. Journal of Sedimentary Research, 71(2): 272−285.

Payne, J. L., Lehrmann, D. J., Follett, D., Seibel, M., Kump, L. R., Riccardi, A., Altiner, D., Sano, H., Wei, J. Y., 2007. Erosional truncation of uppermost Permian carbonates and implications for Permian−Triassic boundary events. GSA Bulletin, 119(7−8): 771−784.

Payne, J. L., Lehrmann, D. J., Wei, J. Y., Knoll, A. H., 2006. The pattern and timing of biotic recovery from the end-Permian extinction on the Great Bank of Guizhou, Guizhou Province, China. Palaios, 21(1): 63−85.

Payne, J. L., Lehrmann, D. J., Wei, J. Y., Orchard, M. J., Schrag, D. P., Knoll, A. H., 2004. Large perturbations of the carbon cycle during recovery from the end-Permian extinction. Science, 305(5683): 506−509.

Pindell, J. L., Drake, C., (eds), 1998. Paleogeographic Evolution and Non-Glacial Eustacy: Northern South America. SEPM Special Publications, 58: 1−324.

Pittet, B., Strasser, A., Mattioli, E., 2000. Depositional sequences in deep-shelf environments: A response to sea-level changes and shallow-platform carbonate productivity (Oxfordian, Germany and Spain). Journal of Sedimentary Research, 70(2): 392−407.

Pratt, B. R., James, N. P., 1986. The St George Group (Lower Ordovician) of western Newfoundland: Tidal flat island model for carbonate sedimentation in shallow epeiric seas. Sedimentology, 33(3): 313−343.

Read, J. F., Goldhammer, R. K., 1988. Use of Fischer plots to define third-order sea-level curves in Ordovician peritidal cyclic carbonates, Appalachians. Geology, 16(10): 895−899.

Read, J. F., Grotzinger, J. P., Bova, J. A., Koerschner, W. F., 1986. Models for generation of carbonate cycles. Geology, 14(2): 107−110.

Ripepe, M., Fischer, A. G., 1991. Stratigraphic rhythms synthesized from orbital variations. In: Franseen, E. K., Watney, W. L., Kendall, C. G. St., Ross, W., (eds). Sedimentary Modeling: Computer Simulations and Methods for Improved Parameter Definition. Kansas Geological Survey Bulletin, 233: 335−344.

Sadler, P. M., 1994. The expected duration of upward-shallowing peritidal carbonate cycles and their terminal hiatuses. GSA Bulletin, 106(6): 791−802.

Schlager, W., 2005. Carbonate Sedimentology and Sequence Stratigraphy. Tulsa: SEPM, 1−200.

Schubert, J. K., Bottjer, D. J., 1995. Aftermath of the Permian-Triassic mass extinction event: Paleoecology of Lower Triassic carbonates in the western USA. Palaeogeography, Palaeoclimatology, Palaeoecology, 116(1−2): 1−39.

Schulz, M., Schäfer-Neth, C., 1997. Translating Milankovitch climate forcing into eustatic fluctuations via thermal deep water expansion: A conceptual link. Terra Nova, 9(5−6): 228−231.

Scotese, C. R., 1994. Early Triassic paleogeographic map. In: Klein, G. D., Beauchamp, B., Baud, A., Chuvashov, B. I., Lopez-Gamundi, O. R., Parrish, J. T., Ross, C. A., Scholle, P. A., Scotese, C. R., Watney, W. L. Introduction: Project Pangea and workshop recommendations. In: Klein, G. D., (ed). Pangea: Paleoclimate, Tectonics, and Sedimentation during Accretion, Zenith and Breakup of a Supercontinent. GSA Special Papers, 288: 7.

Scotese, C. R., Boucot, A. J., McKerrow, W. S., 1999. Gondwanan paleogeography and paleoclimatology. Journal of African Earth Sciences, 28(1): 99−114.

Spencer, R. J., Demicco, R. V., 1989. Computer models of carbonate platform cycles driven by subsidence and eustasy. Geology, 17(2): 165−168.

Tucker, M. E., Wright, V. P., Dickson, J. A. D., 1990. Carbonate Sedimentology. Oxford: Blackwell Science, 1−482.

Twitchett, R. J., Krystyn, L., Baud, A., Wheeley, J., Richoz, S., 2004. Rapid marine recovery after the end-Permian mass-extinction event in the absence of marine anoxia. Geology, 32(9): 805−808.

Wignall, P. B., Hallam, A., 1996. Facies change and the end-Permian mass extinction in S.E. Sichuan, China. Palaios, 11(6): 587−596.

Wignall, P. B., Twitchett, R. J., 1996. Oceanic anoxia and the end Permian mass extinction. Science, 272(5265): 1155−1158.

Wilkinson, B. H., Drummond, C. N., Diedrich, N. W., Rothman, E. D., 1999. Poisson processes of carbonate accumulation on Paleozoic and Holocene platforms. Journal of Sedimentary Research, 69(2): 338−350.

Wilkinson, B. H., Opdyke, B. N., Algeo, T. J., 1991. Time partitioning in cratonic carbonate rocks. Geology, 19(11): 1093−1096.

Woods, A. D., Bottjer, D. J., Mutti, M., Morrison, J., 1999. Lower Triassic large sea-floor carbonate cements: Their origin and a mechanism for the prolonged biotic recovery from the end-Permian mass extinction. Geology, 27(7): 645−648.

Yang, W., Harmsen, F., Kominz, M. A., 1995. Quantitative analysis of a peri-tidal carbonate sequence, the Middle and Upper Devonian Lost Burro Formation, Death Valley, California — A possible Milankovitch climatic record. Journal of Sedimentary Research, 65(3b): 306−322.

Yang, W., Lehrmann, D. J., 2003. Milankovitch climatic signals in Lower Triassic (Olenekian) peritidal carbonate successions, Nanpanjiang Basin, South China. Palaeogeography, Palaeoclimatology, Palaeoecology, 201(3−4): 283−306.

Zempolich, W. G., 1993. The drowning succession in Jurassic carbonates of the Venetian Alps, Italy: A record of super continent breakup, gradual eustatic rise, and eutrophication of shallow-water environments. In: Loucks, R. G., Sarg, J. F. (eds). Carbonate Sequence Stratigraphy: Recent Developments and Applications. AAPG Memoir, 57: 63−105.

(Edited by Xiu-Fang Hu)